Multifractal variability in self-potential signals measured in seismic areas

LUCIANO TELESCA[1], VINCENZO LAPENNA[1] & MARIA MACCHIATO[2]

[1]*Institute of Methodologies for Environmental Analysis, CNR, C.da S.Loja, 85050 Tito (PZ), Italy (e-mail: ltelesca@imaa.cnr.it)*

[2]*Dipartimento di Scienze Fisiche, INFM, Università 'Federico II', Naples, Italy*

Abstract: Multifractal variability in the time dynamics of geoelectrical data, recorded in a seismic area of southern Italy, was studied by means of Multifractal Detrended Fluctuation Analysis (MF-DFA), which allows the detection of multifractality in nonstationary signals. Our findings show that the multifractality of the geoelectrical time series recorded in the study area is mainly due to the different long-range correlations for small and large fluctuations. Furthermore, the singularity spectrum has led to a better description of the signal, revealing a clear enhancement of its degree of multifractality (measured by the variation of the standard deviation of the generalized Hurst exponents $h(q)$ or the Hölder exponents α) in association with the occurrence of the largest earthquake. However, in order to assess significant correlations between large earthquakes and patterns of multifractal parameters, an investigation of data sets covering longer periods and different seismotectonic environments is needed. The study also furnishes details on our approach for investigating the complex dynamics of earthquake-related geoelectrical signals.

Research devoted to investigating earthquakes and earthquake-related geophysical variability has been the subject of growing interest in recent years. Monitoring the time variability of several geophysical parameters may be useful in understanding phenomena linked to seismic activity (Rikitake 1988; Zhao & Qian 1994; Park 1997; Martinelli & Albarello 1997; Di Bello *et al.* 1998; Vallianatos & Tzanis 1999; Hayakawa *et al.* 2000; Telesca *et al.* 2001; Tramutoli *et al.* 2001). In particular, variations in the stress and fluid flow fields can produce changes in the self-potential field (Scholz 1990), which may be used to obtain information on the governing mechanisms both in normal conditions and during intense seismic activity.

Self-potentials are voltage differences between two points on the Earth's surface. These are caused by the presence of an electric field produced by natural sources distributed in the subsoil (e.g. Parasnis 1986; Sharma 1997; and references therein). The most relevant phenomenon that may originate self-potential anomalous fields is known as streaming potential; the electrical signal is produced when a fluid flows in a porous rock, due to a pore pressure gradient. The phenomenon is generated by the formation within the porous ducts of a double electrical layer between the bounds of the solid, which absorbs electrolytic anions and cations distributed in a diffused layer near the boundaries. The dissolved salts increase the amount of anions and cations of the underground liquids. The free liquid in the centre of the rock pore is usually enriched and cations, and anions are usually absorbed on the soil surface in silicate rock. The free pore water carries an excess positive charge, a part of which accumulates close to the solid–liquid interface forming a stable double layer. When the liquid is forced through the porous medium, the water molecules carry free positive ions in the diffusion part of the pore. This relative movement of cations with reference to the firmly attached anions generates the well-known streaming potential (Keller & Frischknecht 1966), which, as suggested by Mizutani *et al.* (1976), may be responsible for the voltage pattern detected at the ground surface before a major earthquake (Patella 1997). In a seismic focal region, the effect could be enhanced due to increasing accumulation of strain, which can cause rock dilatancy (Nur 1972).

Self-potential dynamics could reflect the irregularity and heterogeneity of the crust, within which phenomena generating self-potential fields occur. Therefore, the structure of the self-potential signal could be linked to the structure of the seismic focal zone. In fact, the geometry and the structure of individual fault zones can be represented by a network with an anisotropic distribution of fracture orientations, and consisting of fault-related structures including small faults, fractures, veins and folds. This is a consequence of the roughness of the boundaries between each component and the interaction between the distinct components within the fault zone (O'Brien *et al.* 2003). In

From: CELLO, G. & MALAMUD, B. D. (eds) 2006. *Fractal Analysis for Natural Hazards*. Geological Society, London, Special Publications, **261**, 95–103.
0305-8719/06/$15.00

fact, earthquake faulting is characterized by irregular rupture propagation and non-uniform distributions of rupture velocity, stress drop and coseismic slip. These observations indicate a non-uniform distribution of strengths in the fault zone, whose geometry and mechanical heterogeneity are important factors to be considered in the prediction of strong motion. Experimental studies on the hierarchical nature of the processes underlying fault rupture, leading to the possibility of recognizing the final preparation stage before a large earthquake occurs, have been performed by Lei *et al.* (2003), whereas Cowie *et al.* (1993) introduced a numerical rupture model to simulate the growth of faults in a tectonic plate driven by a constant plate boundary velocity. They found that the plate initially deforms by uncorrelated nucleation of small faults reflecting the distribution of material properties. Because of the increase of strain, the growth and coalescence of existing faults dominate over nucleation, and a power-law distribution of fault size appears, characterizing the fault pattern as fractal. Cowie *et al.* (1995) also show that the combined effect of fault clustering and the correlation between fault displacement and fault size leads to a strongly multifractal deformation pattern.

To characterize quantitatively self-potential (SP) dynamics, techniques able to extract robust features hidden in their complex fluctuations are needed. Fractality is one of the features of such complexity. A fractal is an object whose sample path that is included within some radius r scales with r. Fractal processes are characterized by scaling behaviour, which leads naturally to power-law statistics. Consider $f(x)$, which depends continuously on the scale x over which the measurements are taken. Suppose that changing the scale x by a factor a will effectively scale the statistics $f(x)$ by another factor $g(a)$, $f(ax) = g(a)f(x)$. The only non-trivial solution for this scaling equation is given by $f(x) = bg(x)$, $g(x) = x^c$, for some constants b and c (Thurner *et al.* 1997 and references therein). Therefore, power-law statistics and fractals are very closely related concepts.

The fractality of a signal can be investigated with the aim of characterizing its temporal fluctuations; in this case, we need to perform second-order fractal measurements, which furnish information regarding the correlation properties of a time series. Spectral analysis represents one of the standard methods to detect correlation features in time series fluctuations. The power spectrum is obtained by means of the Fourier transform of the signal. It describes how the power is concentrated at various frequency bands. Thus, the power spectrum reveals periodic, multiperiodic, or non-periodic signals. The fractality of a time series is revealed by a power-law dependence of the spectrum upon the frequency, $S(f) \sim 1/f^{\alpha}$, where the scaling (spectral) exponent α yields information on the type and the strength of the time–correlation structures intrinsic in the signal fluctuations (Havlin *et al.* 1999). If $\alpha = 0$, the temporal fluctuations are purely random, typical of white noise processes, characterized by completely uncorrelated samples. If $\alpha > 0$, the temporal fluctuations are persistent, meaning that variations of the signal will be very likely followed by positive (negative) variations; this feature is typical of systems that are governed by positive feedback mechanisms. If $\alpha < 0$, the temporal fluctuations are antipersistent, meaning that variations of the signal will be very likely followed by negative (positive) variations; this feature is typical of systems that are governed by negative feedback mechanisms.

The estimate of the spectral exponent is rather rough, as a result of large fluctuations in the power spectrum, especially at high frequencies. Furthermore, the power spectrum is sensitive to nonstationarities that could be present in observational data. For this reason, different fractal methods, such as the Higuchi method or detrended fluctuation analysis, have been developed to furnish stable estimates of the spectral exponent (Higuchi 1988, 1990), or to allow the detection of scaling behaviours in experimental time series, very often affected by trends and nonstationarities, which cause spurious detection of correlations (Peng *et al.* 1995).

All the above techniques are monofractal, and very often they are not sufficient to describe the scaling properties of a signal, that could be associated with a multifractal object (i.e. an object that needs many exponents to characterize its scaling properties). In this case, the signal can be decomposed into many subsets characterized by different scaling exponents. Thus, multifractals are intrinsically more complex and inhomogeneous than monofractals, and characterize systems featuring irregular dynamics, with sudden bursts of high-frequency fluctuations.

The aim of the present paper is the dynamical investigation of a self-potential time series recorded in southern Italy, one of the most seismically active areas in the Mediterranean Region. Our purpose is to characterize the multifractality of such time series in order to reveal a possible connection with the seismic activity of the area.

Data

We studied a geoelectrical data set recorded at the Giuliano station (40.688°N, 15.789°E), located in one of the most seismically active areas in southern Italy (Fig. 1). The signal consists of voltage difference between two non-polarizable electrodes

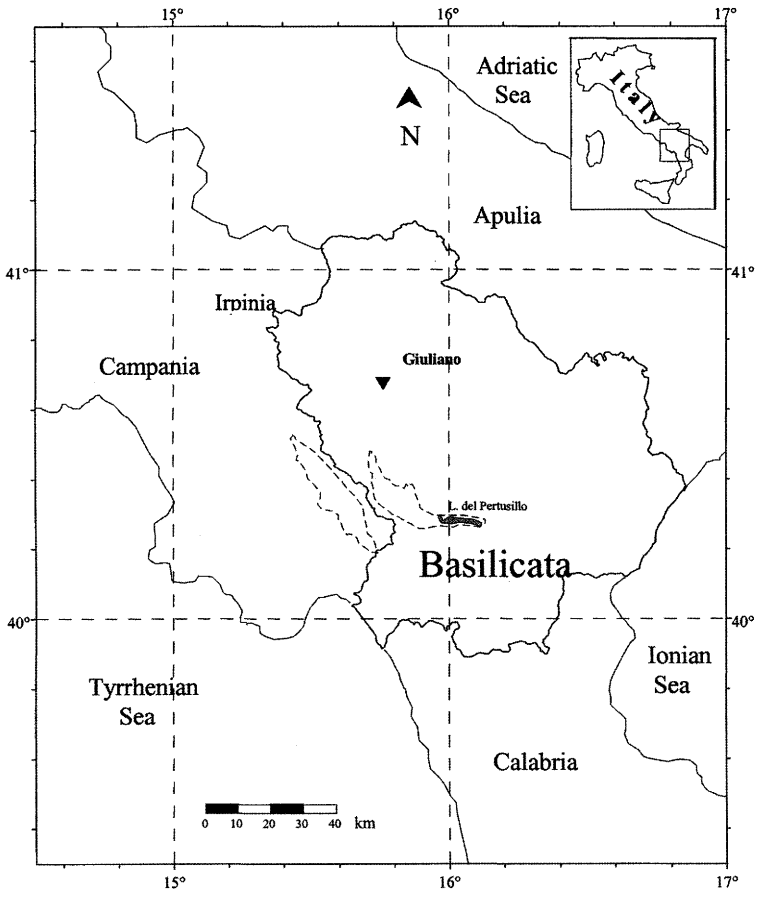

Fig. 1. Location of the Giuliano geoelectrical station in southern Italy. This station has been installed in one of the most seismically active areas of the Mediterranean Region, struck by strong earthquakes in past (1857) and recent years (1980).

inserted 1 m deep in the ground to avoid external temperature effects. The distance between the electrodes was 100 m. Figure 2 shows a time series, which consists of minute-sampled geoelectrical values, recorded from 1 March 2001 to 31 May 2003, and the location of the earthquakes with magnitude $M \geq 3.0$ that occurred in the area during the observation period. These values satisfy Dobrovolsky's rule (Dobrovolsky *et al.* 1979, 1993), which is a theoretical relation between earthquake magnitude, distance from the epicentre, and volumetric strain, and states that detectable seismically induced strain exceeds 10^{-8}. From this relation the maximum distance from the epicentre in which the effects of the earthquake are detectable is $r = 10^{0.43M}$, where r is measured in km. It may be observed, from Figure 2, that the signal shows large fluctuations in association with the occurrence of the selected earthquakes; these are sharper for the largest event ($M = 4.1$) of the seismic sequence.

Methods and data analysis

Observational data often show clear irregular dynamics, characterized by sudden bursts of high-frequency fluctuations. This suggests performing a multifractal analysis in order to detect the possible occurrence of different scaling behaviours for different intensities of fluctuations. Furthermore, the signal may often appear to be nonstationary.

Multifractal Detrended Fluctuation Analysis (MF-DFA) (Kantelhardt *et al.* 2002) is a useful tool to characterize multifractality in nonstationary data. The method is based on the conventional detrended fluctuation analysis (Peng *et al.* 1995).

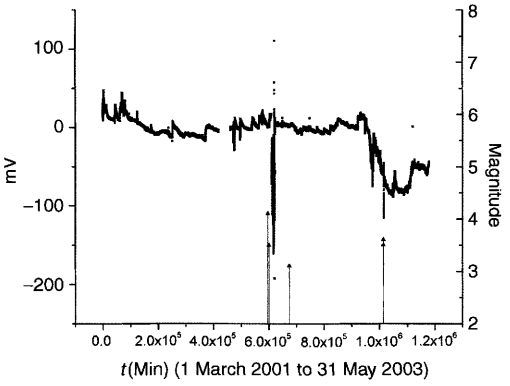

Fig. 2. Time variation of the geoelectrical signal, measured at the Giuliano site, and the earthquakes (vertical arrows) that occurred in the area and satisfy Dobrovolsky's rule (Telesca *et al.* 2004). The signal consists of minute-sampled voltage differences between two non-polarizable electrodes inserted 1 m deep in the ground to avoid external temperature effects. The distance between the electrodes is 100 m and the data were recorded from 1 March 2001 to 31 May 2003.

It operates on the time series $x(i)$, where $i = 1, 2, \ldots, N$ and N is the length of the series. The mean value is indicated by x_{ave}. Assuming that $x(i)$ are increments of a random walk process around the average x_{ave}, the 'trajectory' or 'profile' is given by the integration of the signal

$$y(i) = \sum_{k=1}^{i} [x(k) - x_{\text{ave}}]. \tag{1}$$

Next, the integrated time series is divided into $N_S = \text{int}(N/s)$ non-overlapping segments of equal length s. Because the length N of the series is often not a multiple of the considered time-scale s, a short part at the end of the profile $y(i)$ may remain. In order not to disregard this part of the series, the same procedure is repeated starting from the opposite end. Therefore, $2N_S$ segments are obtained in total. The local trend for each of the $2N_S$ segments is then calculated by a least-square fit of the series. Then one calculates the variance

$$F^2(s,\nu) = \frac{1}{s}\sum_{i=1}^{s} \{y[(\nu-1)s+i] - y_\nu(i)\}^2 \tag{2}$$

for each segment ν, $\nu = 1, \ldots, N_S$ and

$$F^2(s,\nu) = \frac{1}{s}\sum_{i=1}^{s} \{y[N-(\nu-N_S)s+i] - y_\nu(i)\}^2 \tag{3}$$

for $\nu = N_S+1, \ldots, 2N_S$. Here, $y_\nu(i)$ is the fitting line in segment ν. Then, an average over all segments is performed to obtain the qth order fluctuation function

$$F_q(s) = \left\{\frac{1}{2N_S}\sum_{\nu=1}^{2N_S}[F^2(s,\nu)]^{\frac{q}{2}}\right\}^{\frac{1}{q}} \tag{4}$$

where, in general, the index variable q can assume any real value except zero.

Repeating the procedure described above, for several time-scales s, $F_q(s)$ will increase with increasing s. Then, analysing log–log plots $F_q(s)$ v. s for each value of q, the scaling behaviour of the fluctuation functions can be determined. If the series x_i is long-range power-law correlated, $F_q(s)$ increases for large values of s as a power-law

$$F_q(s) \propto s^{h(q)}. \tag{5}$$

The value $h(0)$ corresponds to the limit $h(q)$ for $q \to 0$, and cannot be determined directly using the averaging procedure of Eq. (4) because of the diverging exponent. Instead, a logarithmic averaging procedure has to be employed,

$$F_0(s) \equiv \exp\left\{\frac{1}{4N_S}\sum_{\nu=1}^{2N_S}\ln[F^2(s,\nu)]\right\} \approx s^{h(0)}. \tag{6}$$

In general, the exponent $h(q)$ will depend on q. For stationary time series, $h(2)$ is the well-defined Hurst exponent H (Feder 1988). Thus, we call $h(q)$ the generalized Hurst exponent. Monofractal time series are characterized by $h(q)$ independent of q. The different scaling of small and large fluctuations will yield a significant dependence of $h(q)$ on q. For positive q, the segments ν with large variance (i.e. large deviation from the corresponding fit) will dominate the average $F_q(s)$. Therefore, if q is positive, $h(q)$ describes the scaling behaviour of the segments with large fluctuations, and generally, large fluctuations are characterized by a smaller scaling exponent $h(q)$ for multifractal time series. For negative q, the segments ν with small variance will dominate the average $F_q(s)$. Thus, for negative q values, the scaling exponent $h(q)$ describes the scaling behaviour of segments with small fluctuations, usually characterized by larger scaling exponents.

Two types of multifractality that underlie the q-dependence of the generalized Hurst exponent in time series can be discriminated: (1) due to a broad probability density function for the values of the time series, and (2) due to different long-range

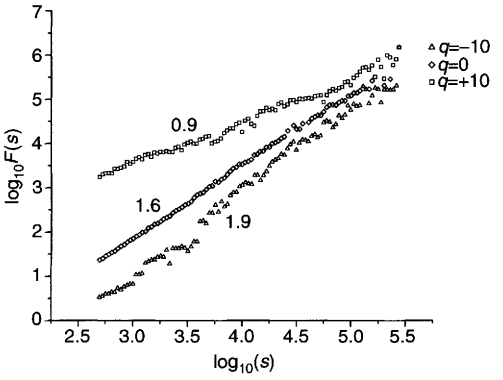

Fig. 3. Fluctuation functions for $q = -10$, 0, 10. The different slopes of the lines fitting the curves by a least-square method suggest the presence of multifractality.

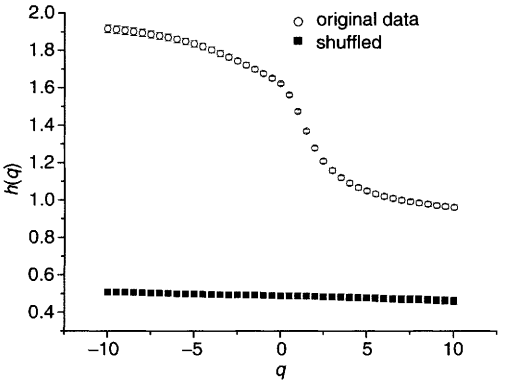

Fig. 4. The $h(q)$–q relation for the original and shuffled series. The difference between the two $h(q)$ spectra is very clear, suggesting that the multifractality of the original signal is significant and depends on the different long-range correlations between small and large fluctuations.

correlations for small and large fluctuations. Both of them need a multitude of scaling exponents for small and large fluctuations. The easiest way to discriminate between these two types of multifractality is by analysing the corresponding randomly shuffled series. In the shuffling procedure the values are put into random order and, although all correlations are destroyed, the probability density function remains unchanged. Hence, the shuffled series coming from multifractals of type (2) will exhibit simple random behaviour with $h_{\text{shuf}}(q) = 0.5$, which corresponds to purely random dynamics. Instead, those coming from multifractals of type (1) will show $h(q) = h_{\text{shuf}}(q)$, because the multifractality depends on the probability density. If both types of multifractality characterize the time series, the shuffled series will show weaker multifractality than the original one.

Figure 3 provides three fluctuation functions $F_q(s)$ ($q = -10$, 0, 10) for the self-potential signal measured at the Giuliano station for time-scales s ranging from 5×10^2 min to $N/4$, where N is the total length of the series. The length of the series ($N \sim 1.2 \times 10^6$) allows us to consider the estimated exponents reliable. The fluctuation functions present different slopes, estimated by a least-square method (the coefficient of correlation is 0.99 in all three cases); this suggests the presence of multifractality in the series. Figure 4 shows the q-dependence of the generalized Hurst exponent $h(q)$ determined by fits in the regime 5×10^2 min $< s < N/4$ and for q ranging between -10 and 10 with 0.5 steps. The generalized Hurst exponents v. q, averaged over 10 randomly shuffled versions of the original time series are also shown. The error bars delimit the $1 - \sigma$ range around the mean values. The $h_{\text{shuf}}(q)$ values range around 0.5, but with a slight q-dependence; this indicates that the multifractality of the self-potential data is mainly due to the different long-range correlations for small and large fluctuations.

The multifractal scaling exponents $h(q)$ defined in Eq. (6) are directly related to the scaling exponents $\tau(q)$ defined by the standard partition function multifractal formalism (Kantelhardt *et al.* 2002). Suppose that the series x_k is a stationary, positive and normalized sequence. Then the detrending procedure of the MF-DFA is not required. Thus the DFA can be replaced by the 'fluctuation analysis' (FA), for which the variance is defined as

$$F^2_{\text{FA}}(s, \nu) = [y(\nu s) - y((\nu - 1)s)]^2. \qquad (7)$$

Inserting this definition into Eq. (4) and using Eq. (6), we obtain

$$\left\{ \frac{1}{2N_S} \sum_{\nu=1}^{2N_S} |y(\nu s) - y((\nu - 1)s)|^q \right\}^{\frac{1}{q}} \approx s^{h(q)}. \qquad (8)$$

For the sake of simplicity, we assume that the length N of the sequence is an integer multiple of the scale s, obtaining $N_S = N/s$ and therefore

$$\sum_{\nu=1}^{N_S} |y(\nu s) - y((\nu - 1)s)|^q \approx s^{qh(q)-1}. \qquad (9)$$

The term $[y(\nu s) - y((\nu - 1)s)]$ is the sum of the numbers x_k within each segment ν of size s. This sum is known as the box probability $p_s(\nu)$ in the standard multifractal formalism for normalized series x_k.

The scaling exponent $\tau(q)$ is usually defined via the partition function $Z_q(s)$,

$$Z_q(s) = \sum_{\nu=1}^{N_S} |p_s(\nu)|^q \approx s^{\tau(q)} \tag{10}$$

where q is a real parameter as in the MF-DFA. Equation (10) is identical to Eq. (9), therefore

$$\tau(q) = qh(q) - 1. \tag{11}$$

In this equation, $h(q)$ is different from the generalized multifractal dimensions $D(q) = \tau(q)/(q-1)$; in fact, although $h(q)$ is independent of q for a monofractal series with compact support, $D(q)$ depends on q in that case (Kantelhardt *et al.* 2002). The assumption of compact support of the series leads to the fractal dimension of the support $D(0) = -\tau(0) = 1$.

Therefore, monofractal series with long-range correlations are characterized by the linearly dependent q-order exponent $\tau(q)$, that is, the exponents $\tau(q)$ of different moments q are linearly dependent on q

$$\tau(q) = Hq - 1 \tag{12}$$

with a single Hurst exponent,

$$H = \mathrm{d}\tau/\mathrm{d}q = \text{const.} \tag{13}$$

Long-range correlated multifractal signals have a multiple Hurst exponent, that is, the generalized Hurst exponent $h(q)$,

$$h(q) = \mathrm{d}\tau/\mathrm{d}q \neq \text{const} \tag{14}$$

where $\tau(q)$ depends nonlinearly on q (Ashkenazy *et al.* 2003).

The singularity spectrum $f(\alpha)$ is related to $\tau(q)$ by means of the Legendre transform (Parisi & Frisch 1985),

$$\alpha = \frac{\mathrm{d}\tau}{\mathrm{d}q} \tag{15}$$

$$f(\alpha) = q\alpha - \tau(q) \tag{16}$$

where α is the Hölder exponent and $f(\alpha)$ indicates the dimension of the subset of the series that is characterized by α. The singularity spectrum quantifies in detail the long-range correlation properties of a time series. Figure 5 shows the multifractal spectrum $f(\alpha)$ for the original and the shuffled series. The spectrum of the original series is completely different from that of the shuffled series, indicating a significant multifractality.

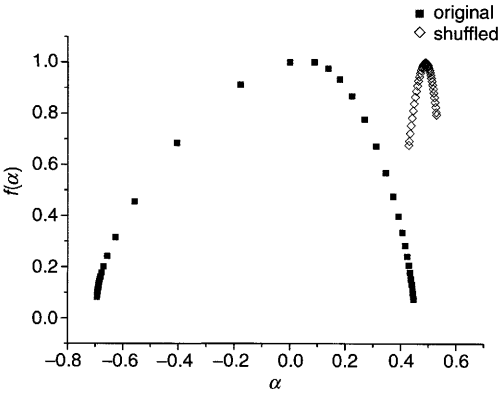

Fig. 5. Singularity spectra of the original and shuffled series. The spectrum of the original series is clearly wider than that of the shuffled series, suggesting a higher multifractality degree.

We investigated the time variation of the multifractal behaviour of the series in order to find possible correlations with the local earthquakes occurring during the observation period. We calculated the set of the generalized Hurst exponent $\{hq(t): -10 \leq q \leq +10\}$ in overlapping time windows 10^5 minutes long; the time shift between two successive windows was set to 5×10^3 min. Figure 6 shows the time variation of the $h(q)$ spectrum; strong variability is clearly visible. Figure 7 shows the time variation of the multifractal

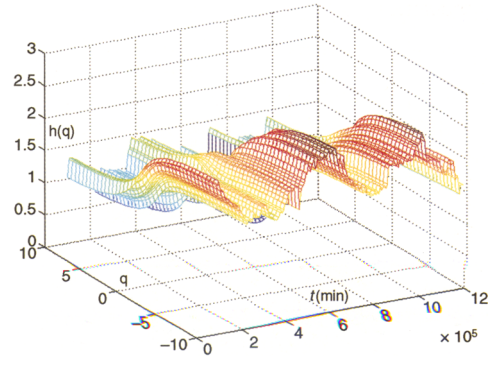

Fig. 6. Time variation of the $h(q)$–q spectrum. The generalized Hurst exponents $\{hq(t): -10 \leq q \leq +10\}$ are calculated in overlapping time windows 10^5 min long; the time shift between two successive windows was set to 5×10^3 min. The strong variability of the $h(q)$ spectrum with time indicates an analogous variability of the multifractality of the signal.

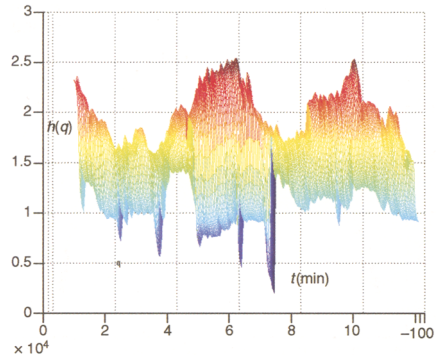

Fig. 7. Time variation of the singularity spectrum $f(\alpha)$. The spectra are obtained from the Legendre transform applied to overlapping time windows 10^5 min long; the time shift between two successive windows was set to 5×10^3 min. The width of the singularity spectrum changes with time, indicating a significant variability of the multifractality of the signal.

spectrum, obtained by the Legendre transform from the $h(q)$ spectrum. The multifractal spectrum also presents a strong variability with time, more visible in the projection on the plane $f(\alpha)-\alpha$ (Fig. 8), which shows a clear enhancement of the range of the α values in association with the occurrence of the largest earthquake (Fig. 9). Figures 10 and 11 show the standard deviation of the $h(q)$ exponents and the α values varying with time (both parameters can be considered a measure of the degree of multifractality of the series); clear enhancement of both parameters is visible in correspondence with the largest earthquake.

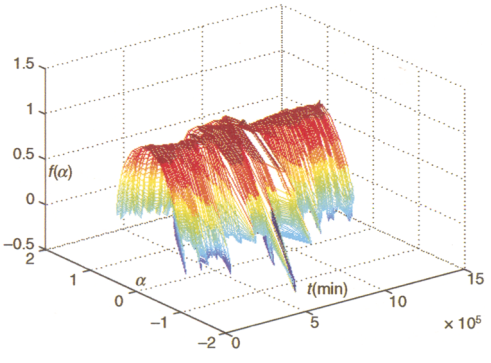

Fig. 8. $f(\alpha)-\alpha$ projection of the graph plotted in Figure 7. This projection clearly shows the variability of the width of the singularity spectrum with time.

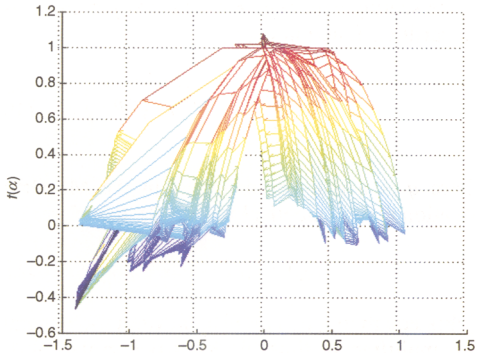

Fig. 9. Time variation of the Hölder α value. A clear enhancement of the range of the α values in association with the occurrence of the largest earthquake ($M = 4.1$) of the recorded seismic sequence is visible.

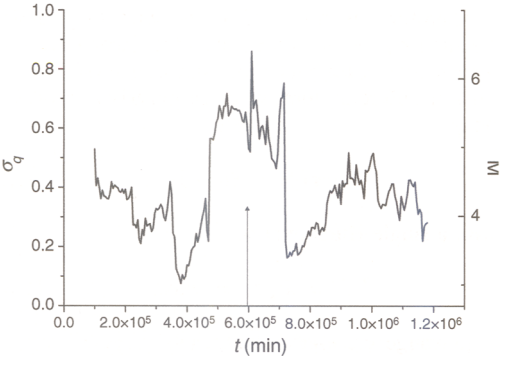

Fig. 10. Time variation of the standard deviation of the $h(q)$ exponents. This parameter can be considered as a measure of the multifractality degree and shows a clear enhancement in correspondence with the largest earthquake.

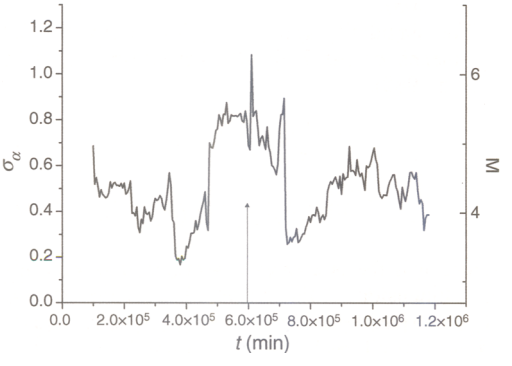

Fig. 11. Time variation of the standard deviation of the Hölder α value. This parameter can be considered as a measure of the multifractality degree and shows a clear enhancement in correspondence with the largest earthquake.

Conclusions

The geophysical phenomenon underlying the self-potential variability connected to earthquake activity is complex and is governed by physical laws that are not completely known. Multifractal analysis has led to a better understanding of such complexity, by means of the generalized Hurst exponents and the singularity spectrum. Using the surrogate series, obtained by a random shuffling procedure, the multifractality of the series is shown to be mainly due to different long-range correlations for small and large fluctuations. The singularity spectrum has led to a better description of the signal, revealing a clear enhancement of its degree of multifractality (measured by the variation of the standard deviation of the generalized Hurst exponents $h(q)$ or the Hölder exponents α) in association with the occurrence of the largest earthquake. In order to assess significant correlations between large earthquakes and patterns of multifractal parameters, and to became more confident in using such patterns to perform feasible earthquake prediction, we need however to investigate data sets covering longer periods, and different seismotectonic environments. The use of multifractal tools is nevertheless promising for better characterizing the time dynamics of earthquake-related geophysical phenomena.

References

ASHKENAZY, Y., HAVLIN, S., IVANOV, P. CH., PENG, C.-K., SCHULTE-FROHLINDE, V. & STANLEY, H. E. 2003. Magnitude and sign scaling in power-law correlated time series. *Physica A*, **323**, 19–41.

COWIE, P. A., VANNESTE, C. & SORNETTE, D. 1993. Statistical physics model for the spatio-temporal evolution of faults. *Journal of Geophysical Research*, **98**, 21809–21821.

COWIE, P. A., SORNETTE, D. & VANNESTE, C. 1995. Multifractal scaling properties of a growing fault population. *Geophysical Journal International*, **122**, 457–469.

DI BELLO, G., HEINICKE, J., KOCH, U., LAPENNA, V., MACCHIATO, M., MARTINELLI, G. & PISCITELLI, S. 1998. Geophysical and geochemical parameters jointly monitored in a seismic area of Southern Apennines (Italy). *Physics and Chemistry of the Earth*, **23**, 909–914.

DOBROVOLSKY, I. P. 1993. Analysis of preparation of a strong tectonic earthquake. *Physics of the Solid Earth*, **28**, 481–492.

DOBROVOLSKY, I. P., ZUBKOV, S. I. & MIACHKIN, V. I. 1979. Estimation of the size of earthquake preparation zones. *Pageoph*, **117**, 1025–1044.

FEDER, J. 1988. *Fractals*. Plenum Press, New York.

HAVLIN, S., AMARAL, L. A. N., ASHKENAZY, Y., GOLDBERGER, A. L., IVANOV, P. CH. PENG, C.-K. & STANLEY, H. E. 1999. Application of statistical physics to heartbeat diagnosis. *Physica A*, **274**, 99–110.

HAYAKAWA, M., HATTORI, K., ITOH, T. & YUMOTO, K. 2000. ULF electromagnetic precursors for an earthquake at Biak, Indonesia on February 17, 1996. *Geophysical Research Letters*, **27**, 1531–1534.

HIGUCHI, T. 1988. Approach to an irregular time series on the basis of the fractal theory. *Physica D*, **31**, 277–283.

HIGUCHI, T. 1990. Relationship between the fractal dimension and the power law index for a time series: a numerical investigation. *Physica D*, **46**, 254–264.

KANTELHARDT, J. W., ZSCHIEGNER, S. A., KONSCIENLY-BUNDE, E., HAVLIN, S., BUNDE, A. & STANLEY, H. E. 2002. Multifractal detrended fluctuation analysis of nonstationary time series. *Physica A*, **316**, 87–114.

KELLER, G. V. & FRISCHKNECHT, F. C. 1966. *Electrical Methods in Geophysical Prospecting*. Pergamon Press, Oxford.

LEI, X., KUSUNOSE, K., NISHIZAWA, O. & SATOH, T. 2003. The hierarchical rupture process of a fault: an experimental study. *Physics of the Earth and Planetary Interiors*, **137**, 213–228.

MARTINELLI, G. & ALBARELLO, D. 1997. Main constraints for siting monitoring networks devoted to the study of earthquake related hydrogeochemical phenomena in Italy. *Annali di Geofisica*, **40**, 1505–1522.

MIZUTANI, H., ISHIDO, T., YOKOKURA, T. & OHNISHI, S. 1976. Electrokinetic phenomena associated with earthquakes. *Geophysical Research Letters*, **3**, 365–368.

NUR, A. 1972. Dilatancy pore fluids and premonitory variations of ts/tp travel times. *Bulletin of the Seismological Society of America*, **62**, 1217–1222.

O'BRIEN, G. S., BEAN, C. J. & MCDERMOTT, F. 2003. A numerical study of passive transport through fault zones. *Earth and Planetary Science Letters*, **214**, 633–643.

PARASNIS, D. S. 1986. *Principles of Applied Geophysics*, Chapman and Hall, London.

PARISI, G. & FRISCH, U. 1985. A multifractal model of intermittency. *In*: GHIL, M., BENZI, R. & PARISI, G. (eds) *Turbulence and Predictability in Geophysical Fluid Dynamics and Climate Dynamics*. North Holland, Amsterdam, 84–88.

PARK, S. K. 1997. Monitoring resistivity changes in Parkfield, California 1988–1995. *Journal of Geophysical Research*, **102**, 24545–24559.

PATELLA, D. 1997. Introduction to ground surface SP tomography. *Geophysical Prospecting*, **45**, 653–681.

PENG, C.-K., HAVLIN, S., STANLEY, H. E. & GOLDBERGER, A. L. 1995. Quantification of scaling exponents and crossover phenomena in nonstationary heartbeat time series. *Chaos*, **5**, 82–87.

RIKITAKE, T. 1988. Earthquake prediction: an empirical approach. *Tectonophysics*, **148**, 195–210.

SCHOLZ, C. H. 1990. *The Mechanics of Earthquakes and Faulting*. Cambridge University Press, New York.

SHARMA, P. S. 1997. *Enviromental and Engineering Geophysics*. Cambridge University Press, Cambridge.

TELESCA, L., CUOMO, V., LAPENNA, V. & MACCHIATO, M. 2001. A new approach to investigate the correlation between geoelectrical time fluctuations and earthquakes in a seismic area of southern Italy. *Geophysical Research Letters*, **28**, 4375–4378.

TELESCA, L., COLANGELO, G., LAPENNA, V. & MACCHIATO, M. 2004. Fluctuation dynamics in geoelectrical data: an investigation by using multifractal detrended fluctuation analysis. *Physics Letters A*, **332**, 398–404.

THURNER, S., LOWEN, S. B., FEURSTEIN, M. C., HENEGHAN, C., FEICHTINGER, H. C. & TEICH, M. C. 1997. Analysis, synthesis, and estimation of fractal-rate stochastic point processes. *Fractals*, **5**, 565–596.

TRAMUTOLI, V., DI BELLO, G., PERGOLA, N. & PISCITELLI, S. 2001. Robust satellite techniques for remote sensing of seismically active areas. *Annali di Geofisica*, **44**, 295–312.

VALLIANATOS, F. & TZANIS, A. 1999. On possible scaling laws between Electric Earthquake Precursors (EEP) and Earthquake Magnitude. *Geophysical Research Letters*, **26**, 2013–2016.

ZHAO, Y. & QIAN, F. 1994. Geoelectric precursors to strong earthquakes in China. *Tectonophysics*, **233**, 99–113.